ARCHIVIO ISTITUZIONALE
DELLA RICERCA

Alma Mater Studiorum Università di Bologna
Archivio istituzionale della ricerca

Irradiation and performance of RGB-HD Silicon Photomultipliers for calorimetric applications

This is the final peer-reviewed author's accepted manuscript (postprint) of the following publication:

Published Version:
Acerbi F., Ballerini G., Berra A., Brizzolari C., Brunetti G., Catanesi M.G., et al. (2019). Irradiation and performance of RGB-HD Silicon Photomultipliers for calorimetric applications. JOURNAL OF INSTRUMENTATION, 14(2), 1-13 [10.1088/1748-0221/14/02/P02029].

Availability:
This version is available at: https://hdl.handle.net/11585/744910 since: 2020-03-02

Published:

DOI: http://doi.org/10.1088/1748-0221/14/02/P02029

Terms of use:

Some rights reserved. The terms and conditions for the reuse of this version of the manuscript are specified in the publishing policy. For all terms of use and more information see the publisher's website.

This item was downloaded from IRIS Università di Bologna (https://cris.unibo.it/).
When citing, please refer to the published version.

(Article begins on next page)

16 September 2026

This is the final peer-reviewed accepted manuscript of:

F. Acerbi et al., Irradiation and performance of RGB-HD Silicon Photomultipliers for calorimetric applications, Journal of Instrumentation, 2019, vol. 14, article P02029.

The final published version is available online at: http://dx.doi.org/10.1088/1748-0221/14/02/P02029

Rights / License:

The terms and conditions for the reuse of this version of the manuscript are specified in the publishing policy. For all terms of use and more information see the publisher's website.

Prepared for submission to JINST

Irradiation and performance of RGB-HD Silicon Photomultipliers for calorimetric applications

F. Acerbi,[a] **G. Ballerini,**[b,c] **A. Berra,**[b,c] **C. Brizzolari,**[b,c] **G. Brunetti,**[d] **M.G. Catanesi,**[e] **S. Cecchini,**[f] **F. Cindolo,**[f] **A. Coffani,**[c,g] **G. Collazuol,**[d,h] **E. Conti,**[d] **F. Dal Corso,**[d] **C. Delogu,**[c,g] **G. De Rosa,**[i] **A. Gola,**[a] **R. A. Intonti,**[e] **C. Jollet,**[l,m] **Y. Kudenko,**[n] **A. Longhin,**[d,h] **L. Ludovici,**[p] **L. Magaletti,**[i] **G. Mandrioli,**[f] **A. Margotti,**[f] **V. Mascagna,**[b,c] **N. Mauri,**[f,o] **A. Meregaglia,**[m] **M. Pari,**[d,h] **L. Pasqualini,**[f,o] **G. Paternoster,**[a] **L. Patrizii,**[f] **C. Piemonte,**[a] **M. Pozzato,**[f] **F. Pupilli,**[d] **M. Prest,**[b,c] **E. Radicioni,**[e] **C. Riccio,**[i] **A.C. Ruggeri,**[i] **C. Scian,**[h] **G. Sirri,**[f] **M. Soldani,**[b,c] **M. Tenti,**[c,g] **M. Torti,**[c,g] **F. Terranova,** [c,g,1] **E. Vallazza**[q]

[a] *Fondazione Bruno Kessler, Via Sommarive 18, Povo (TN), Italy*
[b] *Università degli Studi dell'Insubria, Via Valleggio 11, Como, Italy*
[c] *INFN Milano Bicocca, Piazza della Scienza 3, Milano, Italy*
[d] *INFN Padova, Via Marzolo 8, Padova, Italy*
[e] *INFN Sezione di Bari, Via E. Orabona 4, Bari, Italy*
[f] *INFN Sezione di Bologna, Via Berti Pichat 6, Bologna, Italy*
[g] *Università degli Studi di Milano Bicocca, Piazza della Scienza 3, Milano, Italy*
[h] *Università degli Studi di Padova, Via Marzolo 8, Padova, Italy*
[i] *INFN Napoli and Università degli Studi di Napoli, Via Cintia, Napoli, Italy*
[l] *Institute Pluridisciplinaire Hubert Curien, 23 rue du Loess, Strasbourg, France*
[m] *Centre de Etudes Nucleaires de Bordeaux Gradignan, 19 Chemin du Solarium, Bordeaux, France*
[n] *Institute for Nuclear Research of the Russian Academy of Sciences, Moscow, Russia*
[o] *Università degli Studi di Bologna, Via Irnerio 46, Bologna, Italy*
[p] *INFN Roma, Piazzale Aldo Moro 2, Roma, Italy*
[q] *INFN Trieste, Padriciano 99, 34012 Trieste, Italy*

E-mail: francesco.terranova@cern.ch

arXiv:1901.08430v1 [physics.ins-det] 24 Jan 2019

[1] Corresponding author.

Abstract: Silicon Photomultipliers with cell-pitch ranging from 12 μm to 20 μm were tested against neutron irradiation at moderate fluences to study their performance for calorimetric applications. The photosensors were developed by FBK employing the RGB-HD technology. We performed irradiation tests up to 2×10^{11} n/cm^2 (1 MeV eq.) at the INFN-LNL Irradiation Test facility. The SiPMs were characterized on-site (dark current and photoelectron response) during and after irradiations at different fluences. The irradiated SiPMs were installed in the ENUBET compact calorimetric modules and characterized with muons and electrons at the CERN East Area facility. The tests demonstrate that both the electromagnetic response and the sensitivity to minimum ionizing particles are retained after irradiation. Gain compensation can be achieved increasing the bias voltage well within the operation range of the SiPMs. The sensitivity to single photoelectrons is lost at $\sim 10^{10}$ n/cm^2 due to the increase of the dark current.

Keywords: Calorimeters, Photon detectors for UV, visible and IR photons (solid-state), Neutrino detectors, Radiation damage to detector materials (solid state)

Contents

1 Introduction **1**

2 Irradiation tests at LNL **2**

3 Characterization of the irradiated SiPMs **5**

4 Tests on the T9 beamline **7**

5 Conclusions **11**

1 Introduction

The possibility to use compact Silicon Photomultipliers (SiPMs) embedded in the bulk of particle detectors is extremely appealing. Direct coupling with scintillator or wavelength shifter (WLS) fibers [1, 2] remove the inefficiencies and dead areas introduced by the light extraction toward conventional photomultipliers (PMTs). Modern SiPMs are replacing PMTs in a vast number of applications but the operation of these devices in radiation harsh environments remains a challenge [3–7]. Accelerator neutrino physics applications as developed by the ENUBET Collaboration [8] are in between low-dose environments where damage due to non-ionizing particles is small ($< 10^8$ n/cm^2) [9] and high radiation environment as in the forward region of high-luminosity colliders ($> 10^{13}$ n/cm^2) [10]. In ENUBET, compact calorimeters are employed to monitor lepton production in the decay tunnel of neutrino beams at single particle level and to provide a 1% measurement of the neutrino flux at source. The monitored neutrino beams [11] are narrow band beams where particles in the tunnel are recorded only at large angles to identify the decay product of kaons. As a consequence, particle rates and doses are mostly due to hadron interactions.

The integrated fluences to achieve a 1% measurement of the ν_e and ν_μ cross sections depend on the position of the calorimeter with respect to the axis of the secondary beam (mostly pions and kaons) at the entrance of the decay tunnel. Both ionizing radiation doses and non-ionizing radiation fluencies are depicted in Fig. 1 as a function of the distance between the beam axis and the calorimeter. For ENUBET (1 m distance) the non-ionizing fluence integrated during the lifetime of the experiment and scaled to 1 MeV equivalent neutrons is 1.8×10^{11} n/cm^2. The ionizing dose is 0.06 kGy.

The ENUBET calorimeter is an assembly of Ultra Compact Modules (UCM - Fig. 2). The basic module is an iron-plastic scintillator device whose light is collected by WLS fibers running perpendicularly to the absorber and converter plates ("shashlik" calorimeter [12, 13]). In a UCM, every single fiber segment is directly connected to a SiPM [14]. The array of SiPMs reading the UCM is hosted on a PCB (Printed Circuit Board) holder that integrates both the passive components and the signal routing toward the front-end electronics. The calorimeters are assembled grouping arrays

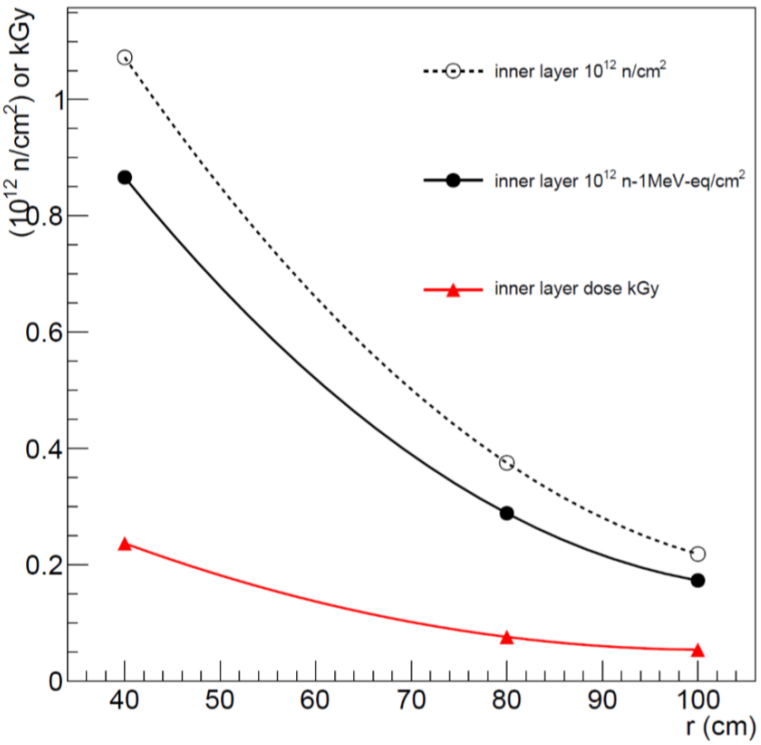

Figure 1: Ionizing doses (in kGy) and non-ionizing fluences (black dashed line: n/cm^2; black continuous line: 1 MeV-equivalent n/cm^2) as a function of the distance between the axis of the ENUBET decay tunnel and the inner radius of the calorimeter.

of UCMs, whose size and thickness (in radiation lengths, X_0) are optimized for the identification of positrons from $K^+ \to e^+\pi^0\nu_e$. In ENUBET, the use of compact calorimetric modules is a very effective solution but results into exposing the SiPMs to fast neutrons produced by hadronic showers. The SiPM technology of choice for ENUBET is RGB-HD: the red-green-blue (sensitivity) - high density technology [15] developed by FBK for small (< 25 µm) pixel sensors with a sensitive area of the same size of the ENUBET wavelength shifter fibers (1 mm^2). This setup has been successfully tested with non-irradiated SiPMs and is described in [16]. In 2017, the RGB-HD sensors were exposed to fast neutrons at the Irradiation Test facility of INFN-LNL (Sec. 2). In Sec. 3 we describe the analysis of the dark current and noise waveform recorded after irradiation at different fluences. The SiPMs were irradiated in the same PCB boards used for the UCM and were tested at CERN to establish the response to minimum ionizing particles (mips) and electrons. The testbeams were performed at the CERN East Area facility (T9 beamline) and are summarized in Sec. 4.

2 Irradiation tests at LNL

The INFN-LNL (Laboratori Nazionali di Legnaro) provides a general purpose irradiation facility based on the CN van der Graaf accelerator [17]. The van der Graaf has a maximum voltage of 7 MV and can accelerate protons and other light nuclei up to 5 μA currents. The tests were performed with a beam of protons impinging on a thick Beryllium target. Neutrons are produced

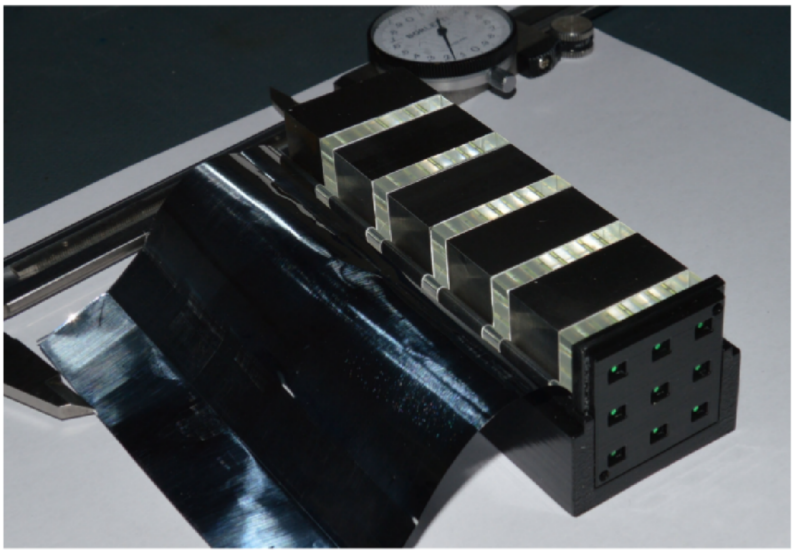

Figure 2: Picture of an ENUBET UCM employed for cosmic ray tests: the PCB hosting the SiPMs is not mounted and the plastic mask holding the fibers is visible in the back of the detector. The PCB (see Fig. 5 below) is then mounted on the mask to couple the fibers to the photonsensors.

by Be(p,xn) reactions, namely ^{9}Be(p,n)^{9}B, ^{9}Be(p,np) 2α, ^{9}Be(p,np)^{8}Be and ^{9}Be(p,nα)^{5}Li. The irradiated sample is located inside an experimental area with an external shield of concrete and an inner shell of water as neutron moderator (see Fig. 3).

A detailed assessment of neutron yields for this beamline has been performed in [18]. The neutron flux in the forward direction is peaked at about 0.5 and 2.7 MeV for 5 MeV protons impinging on the target. Fig. 4 shows the neutron yield per unit current (neutrons/MeV/μC/sr) at different angles (from $\theta = 0^{\circ}$ up to $\theta = 120^{\circ}$). The expected fluxes on the irradiated samples were evaluated from [18] and from the real-time monitoring of the proton current to the target performed with a current integrator. Other effects not included in [18] (neutron backscattering in the shielding toward the sample) were estimated using FLUKA 2011 [19, 20] and give a negligible contribution to the integrated fluence on the sample.

Figure 3: (left) Top view of the irradiation test area at INFN-LNL: the sample holder (on the right) is located in front of the beam-pipe that hosts the Be target. (right) Experimental area and the setup to record the dark current and the waveform of the SiPMs between two irradiation sessions.

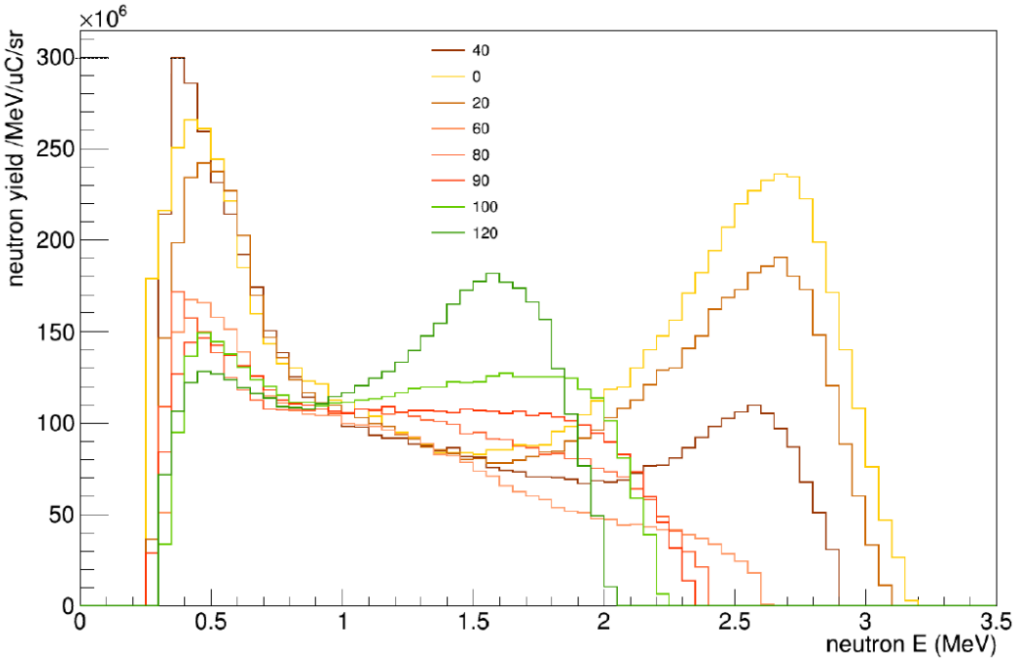

Figure 4: Neutron yield as a function of energy (MeV) at different neutron emission angles (in degrees). Data from [18].

We irradiated three PCB boards used for the ENUBET UCMs. Each board hosts 9 SiPMs and integrates both the passive components and the signal routing toward the front-end electronics. The boards host 20, 15 and 12 µm cell-pitch SiPMs, respectively. The SiPMs belonging to the same UCM are connected in parallel and read out without amplification through a 470 pF decoupling capacitor. The PCB is equipped with a MCX connector to read the sum of the current of the SiPMs and a miniature push-pull coaxial connector (LEMO-00) for the bias. In addition, we assembled a test PCB with a single 1 mm^2, 12 µm pitch SiPM. Between two irradiation sessions, the signal of the test PCB was connected to an Advansid trans-impedance amplifier (ASD-EP-EB-N [21]) and the noise waveforms were recorded by a Rohde & Schwarz RTO 1024 oscilloscope to evaluate the single photoelectron sensitivity. The current as a function of the overvoltage was measured as voltage drop through a 10 kΩ resistor recorded by a Keithley 2700 multimeter and read out by a PC through a Keithley 7702 channel multiplexer. The current of the SiPMs below the breakdown voltage was $O(10^{-9}\text{A})$ for each SiPM and it was measured with a Keithley 485 Picoammeter. The temperature of the sample during irradiation was measured with LM35 temperature sensors recorded by an Arduino One microcontroller board.

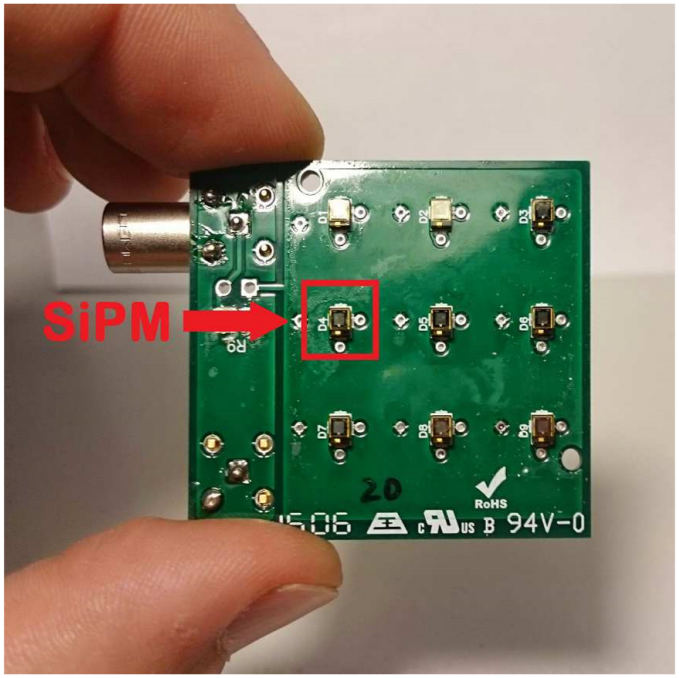

Figure 5: One of the irradiated PCB with the SiPMs and the bias connector already installed.

3 Characterization of the irradiated SiPMs

The three PCBs hosting 9 SiPMs and the single-SiPM PCB were irradiated from a minimum dose of 1.8×10^8 n/cm^2 up to 1.7×10^{11} n/cm^2. During irradiation the SiPMs were not biased and after each irradiation run, several current scans as a function of voltage (I-V curve) were recorded. During the irradiation tests we employed two temperature probes with a precision of 0.5°C. The first one ("room temperature probe") was used to monitor room temperature (25 °C during all the irradiation period), and the second one ("sample probe") was in thermal contact with the irradiated sample. During irradiation, the SiPMs were not biased and only the temperature of the sample was recorded. The maximum increase of temperature during each irradiation run was +10 °C and the sample reached room temperature after 15-30 minutes. The measurements reported below have been recorded when the sample probe reached the value of the room-temperature probe.

Fig. 6 shows the I-V curves for the single-SiPM PCB (1 mm^2 area, 12 µm cell-pitch). The curves were recorded with the sample at room temperature and, in the longest run (from 8.7×10^{10} to 1.7×10^{11} n/cm^2), thermal equilibrium was reached 30 minutes after the stop of the proton beam. The corresponding curves normalized to a single SiPM for the 20 µm cell-pitch PCB are shown in Fig. 7. The normalization is performed dividing the value of the current from the PCB by the number of SiPMs hosted in the board (i.e. 9). The current of all the 20 µm pitch SiPMs was measured with a pico-ammeter before irradiation and is ~ 0.5 nA at 27 V. The I-V curve of the 12 µm cell-pitch PCB hosting 9 SiPMs is consistent with the corresponding single-SiPM PCB, i.e. the current is 9× higher. All the RGB-HD SiPMs show minor changes in the breakdown voltage. For the 12 µm cell-pitch SiPM the breakdown voltage measured at the maximum of $I^{-1}dI/dV$ is 28.2 V for no irradiation and 28.0 V after an exposure of 1.7×10^{11} n/cm^2. As expected, the dark current

after breakdown increases by more than two orders of magnitude at a fluence of $\sim 10^{11}$ n/cm^2. Fig. 8 shows the dark current normalized to 1 SiPM versus fluence at 33 V (+4.8 V overvoltage).

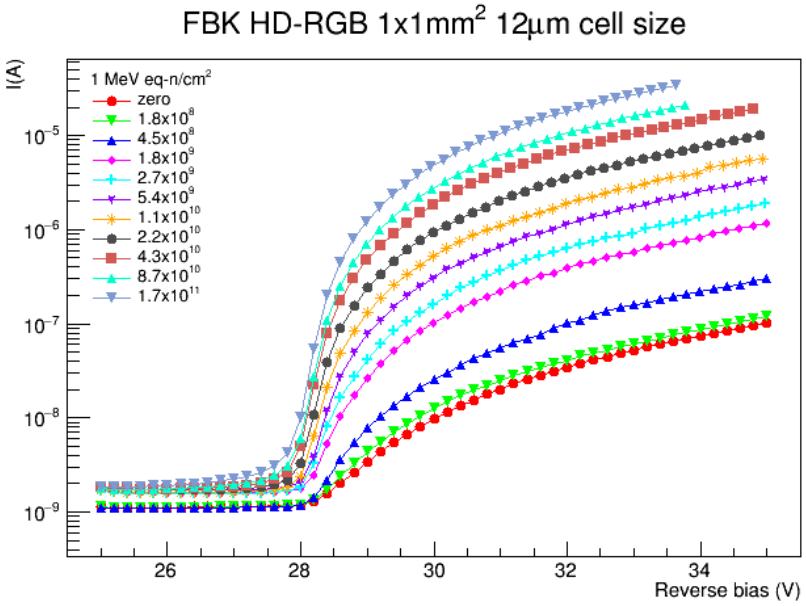

Figure 6: I-V curve of the single-SiPM PCB.

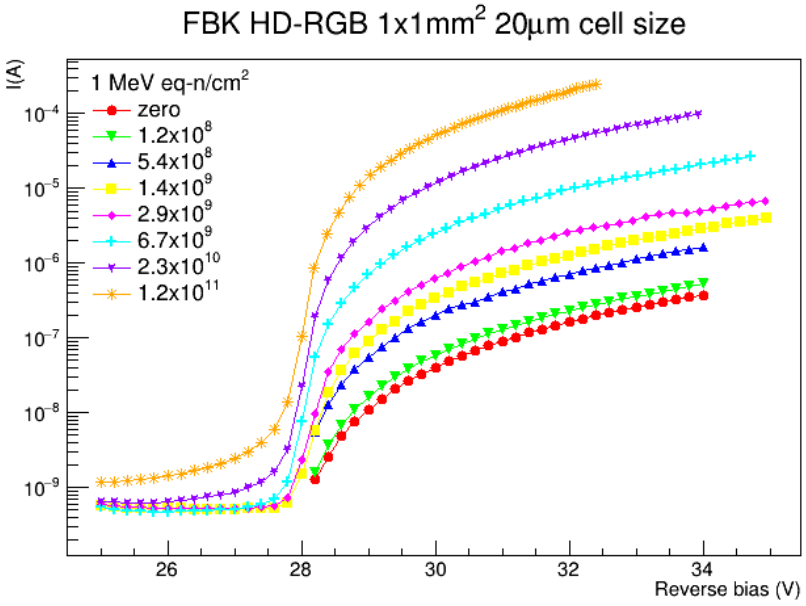

Figure 7: I-V curve of the 20 µm cell-pitch SiPMs. The value shown in the plot is normalized to one SiPM, i.e. the current from the PCB is divided by the number of SiPMs hosted in the board (9 SiPMs per board).

After each irradiation run, the signal terminals of the 12 µm cell-pitch photosensor in the

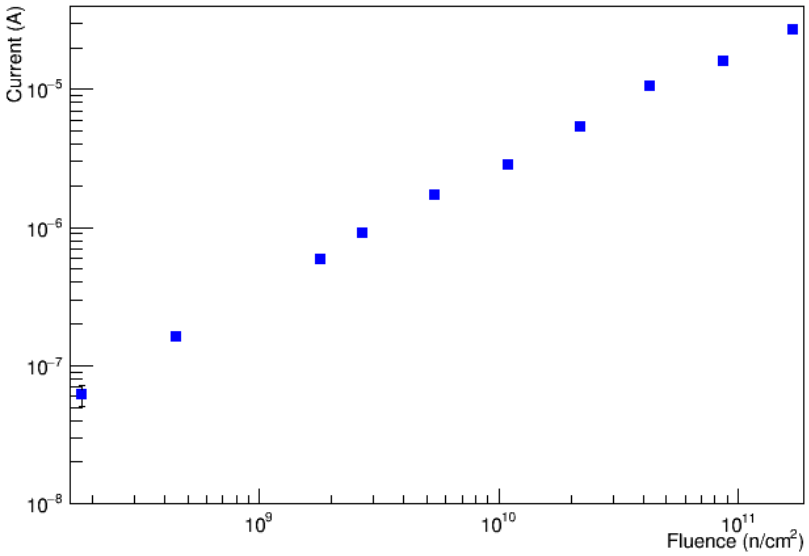

Figure 8: Dark current of the 12 µm cell-pitch SiPMs (current of a 9 SiPM PCB divided by 9) as a function of the neutron fluence. The bias of the SiPMs is 33 V, corresponding to +4.8 V overvoltage.

single-UCM PCB were connected to the OUT2 of the ASD-EP-EB-N amplifier (transimpedance gain: 2500 for a 50 Ω load resistence) and the amplified waveform was recorded by the Rohde & Schwarz oscilloscope. The signal per photoelectron (p.e.) was estimated operating the oscilloscope in self-triggering mode and setting the threshold below the single photoelectron peak. The waveform was sampled for 100 ns at 10 GS/s, i.e. we recorded 1000 samples every 100 ps for each triggered event. The distribution of the signal peak is shown in Fig. 9 at 3×10^9 (left) and 1.2×10^{10} (right) n/cm^2. The three fitted peaks correspond to 1, 2 and 3 p.e. The sensitivity to single photoelectron is lost at fluences larger than 3×10^9 n/cm^2.

After irradiation the samples were stored at 25±1 °C for about three months before installing the boards on the UCM at CERN. In this period, we expect the current to further decrease due to room temperature self-annealing [22] and to reach a plateau with a time constant of about 10 days. We have not studied the behaviour of the dark current versus time during the storage period and, hence, we do not report results on long-term self-anneling for the HD-RGB. Before installation (see Sec. 4), however, we recorded the I-V curves and observed a current reduction comparable to what reported in [22].

4 Tests on the T9 beamline

The irradiated PCBs were tested on the T9 beamline [23] of the CERN East Area facility in October 2017 together with other ENUBET prototypes. Figure 10 shows a schematics of the instrumentation in the beam area. The particle beam is composed of electrons, muons and pions and the momentum can be selected between 1 and 5 GeV, thus covering the whole range of interest for ENUBET. A

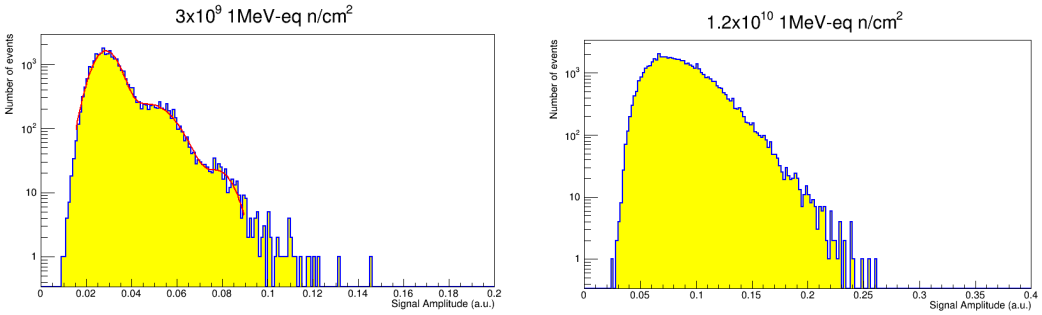

(a) (b)

Figure 9: Signal peak distribution at (a) 3×10^9 and (b) 1.2×10^{10} n/cm^2 for the single-SiPM PCB (12 µm cell-pitch, 1 mm^2 SiPM).

pair of threshold Cherenkov counters filled with CO_2 were used to separate electrons from heavier particles. The acquisition was triggered by a 10×10 cm^2 plastic scintillator located downstream the Cherenkov detectors. We used a pair of silicon strip detectors with a spatial resolution of ~30 μm to track charged particles down to the UCM. Two pads of plastic scintillator ("muon catcher") interleaved by a 20 cm thick iron shield were positioned after the prototypes to identify muons or non-interacting pions. The prototypes under test were positioned inside a light-tight metallic box and mounted on a movable platform in front of the two silicon strip detectors. During the testbeam at CERN, the temperature was monitored by probes placed inside the box containing the calorimeter. In order to stabilize the temperature, we equipped the box with a water-cooled chiller controlled by the probe in termal contact with the UCM. The average temperature during the measurement was 26°C and the maximum variation was ±1°C.

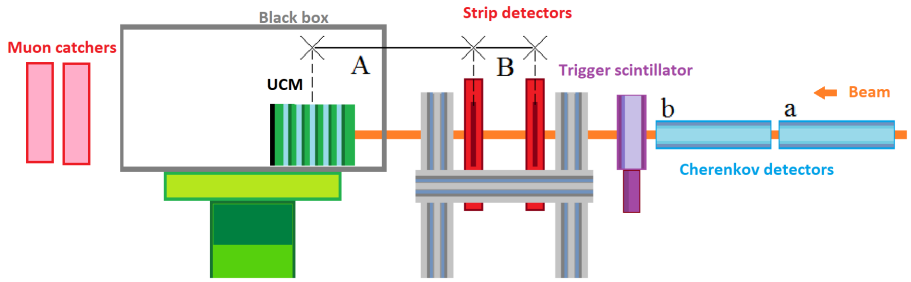

Figure 10: Schematics of the experimental setup at CERN (T9 beamline at the East Area)

Most of the tests were performed using the 15 µm cell-pitch PCB irradiated up to 1.2×10^{11} n/cm^2. The same UCMs were equipped with a non-irradiated PCB identical to the irradiated one. The SiPMs of the two PCBs belong to the same production batch and differences in the breakdown voltage are less than 0.1 V. The PCBs were tested with two ENUBET UCMs:

- **Prototype 16B** This is the first UCM prototype of ENUBET (Fig. 2) and its design was employed for the calorimeter studied in [16]. The UCM was assembled using five 3×3 cm^2 iron slabs with 1.5 cm thickness interleaved by five scintillator tiles (0.5 cm thickness). The slabs were drilled with a CNC machine: the distance between holes was 1 cm and

the diameter of the holes was 1.2±0.2 mm. After drilling, the slabs were zinc-plated to prevent oxidation. The 0.5 thick 3×3 cm^2 scintillator tiles were machined and polished from EJ-200 [24] plastic scintillator sheets and we inserted Tyvek foils between the scintillator and absorber tiles to increase the light collection efficiency. For 16B, we employed 1 mm diameter Kuraray Y11 fibers with an emission peak at 476 nm [25]. Laboratory tests on 16B show that a mip crossing the whole 16B UCM releases about 50 photoelectrons. The number of photoelectrons includes the efficiency of light production, light trasport to the photosensor and the photon detection efficiency (PDE) of the SiPM.

- **prototype 17UA** was built from injection molded scintillator tiles produced by Uniplast (Russia) [26] for ENUBET. In this prototype each tile is made by 3 extruded scintillator slabs (3×3 cm^2, 4.5 mm thickness) for a total thickness of 1.35 cm. The scintillator is polystyrene-based with 1.5% paraterphenyl (PTP) and 0.01% POPOP. The surface of each tile was etched with a chemical agent to form a 30-100 μm layer that acts as a diffusive reflector in order to increase the light collection. The grooves in the mould form the holes for the 1-mm diameter WLS fibers. The UCM was assembled from five 1.5 cm iron slabs interleaved by five 1.35 cm scintillator tiles. As for 16B, we employed Kuraray Y11 fibers since the light emission spectrum of the Uniplast scintillator is similar to EJ-200 and Y-11 are properly matched to both of them. Laboratory tests on 17UA performed in the same conditions as for 16A show that a mip crossing the whole 17UA UCM releases ~85 photoelectrons.

These prototypes were tested using both a 9-SiPM board that was not irradiated at INFN-LNL and an irradiated board. The boards were equipped with 15 μm cell-pitch SiPMs. The irradiated board hosts a SiPM located in the top-right corner that was damaged before the irradiation and that was disconnected during the measurements. This board hence reads 8 active SiPMs.

Electrons were selected requiring a signal in both Cherenkov counters. Mip-like particles (muons or non-interacting pions) correspond to events with no signal in the Cherenkov counters and signal in the muon catcher. The silicon strip detectors are employed to select particles entering the front face of the UCM in a 2×2 cm^2 fiducial area and crossing the whole UCM. Fig. 11 shows the signal response of 16B for mips (green line) and electrons (red line). The left (right) plot corresponds to the UCM with the non-irradiated (irradiated) SiPMs. The black line show all signals triggered during the run and it is dominated by dark counts. The loss of p.e. due to the missing SiPM was computed using a GEANT4 [27–29] optical simulation of the ENUBET UCMs. The average p.e. loss due to the missing SiPM for the particles selected in the fiducial area amounts to 10.6 ± 0.1% (i.e. $\sim 1/9$). A single UCM has a radiation length of 4.3 X_0 and covers 0.9 Moliere radii for particles entering at the center of the front face. In the 1-3 GeV energy range, the first UCM hit by the electrons is also the UCM with the maximum energy deposit although electrons are only partially contained in the UCM and the width of the electron peak is dominated by energy leakage. The signal of the first UCM for mip and electrons (see Fig. 11 and 12) thus provides the detector response in the whole dynamic range of interest for ENUBET.

The results of Fig. 11 demonstrate that a UCM collecting 50 photoelectrons per mip is not able to separate a mip from the noise peak up to the maximum fluence expected in ENUBET (2×10^{11} n/cm^2) due to the increase of the dark counts, even if the electron peak remains well separated from noise. Preserving the sensitivity to mips for the entire duration of the run is important

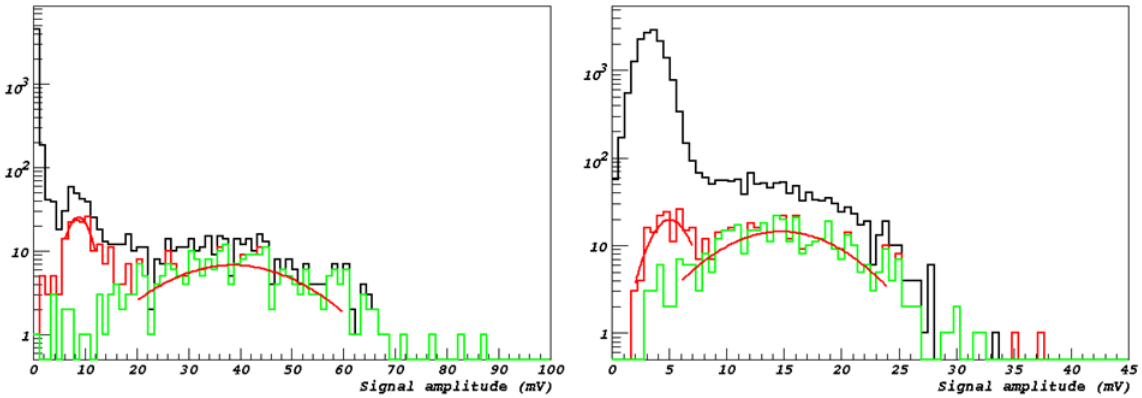

Figure 11: Signal in 16B of electrons (red) and mips (green) measured with the not-irradiated (left) and irradiated (right) PCB. The black line corresponds to all triggers and is dominated by dark noise (see text). The red lines show the Gaussian fit of the signal peak for electrons and mip-like particles. The SiPM overvoltage is +8.8 V and the beam momentum is 1 GeV.

in ENUBET for calibration purposes. The mip signal is employed to monitor changes of the UCM response over the run - complementing the LED monitoring system, - so that signal equalization over time can be achieved increasing the overvoltage to compensate for amplitude losses. In 16B, the number of photoelectrons per mip was limited to the poor fiber-to-SiPM coupling, i.e. the mechanical tolerances in the plastic mask that holds the fibers and couples them to the PCB. Since the fiber diameter has the same size of the width of the SiPM (1 mm), the photon collection efficiency is affected by misalignments between the photosensors and fibers.

The 17UA prototype employs the same SiPM-to-fiber coupling scheme as 16B but has a larger scintillator thickness and the mip peak is separated from the dark noise peak even after irradiation. This is demonstrated in Fig. 12 for 1 GeV particles selected as in 16B. The ratio between the mip peak after and before irradiation is shown in Fig. 13 (top plot) and is corrected for the missing SiPM in the irradiated board. The bottom plot shows the corresponding ratio for electrons at different energies. The overall gain reduction is independent of the particle type, energy and overvoltage within 5%. The electron and mip peak mean value ratio is constant after irradiation and the integrated neutron fluence does not affect the dynamic range of the photosensors. Hence, for the SiPMs employed in this test (pixel size: 15 μm, fill factor: 62%, pixel density: 4444 pixels/mm^2) saturation effects of the signal due to the reduction of the number of working pixels after irradiation are not visible at $O(10^{11}\text{n/cm}^2)$. These effects may become important at fluences of relevance for collider experiments where the choice of the pixel size (smaller pixels to achieve the largest number of cells per unit area) is a critical parameter [3].

Irradiation effects contribute to signal losses through a reduction of the gain×PDE and of the transparency of the epoxy employed for the encapsulation of the SiPM. In this experimental setup, however, non-irradiation effects due to board-to-board variations in the SiPM-to-fiber coupling are sizable (20%) and originate from the fact that the width of the photosensor (1 mm) is the same as the diameter of the WLS fiber. As a consequence, the coupling is sensitive to mechanical displacement of the photosensors [16]. In fact, the signal loss of Fig. 13 represents a conservative estimate of

the change of response during the ENUBET data taking. A signal reduction down to 50% can be recovered by increasing the bias voltage to +5 V, well within the operation range of the SiPM.

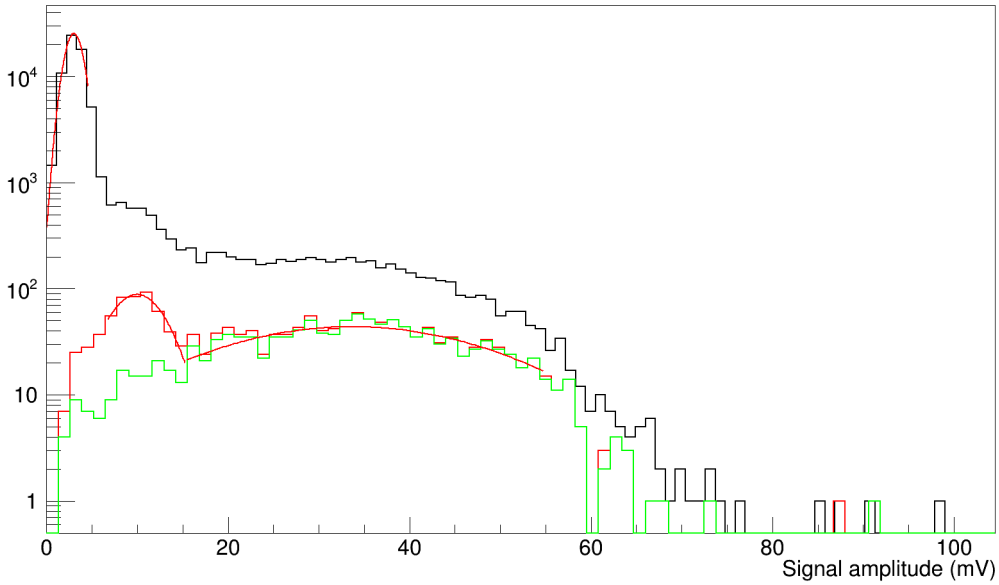

Figure 12: Electron (red) and mip (green) signal in 17UA with irradiated SiPM. The black line corresponds to all triggers and is dominated by dark noise (see text). The SiPM overvoltage is +8.8 V and the beam momentum is 1 GeV.

5 Conclusions

RGB-HD SiPMs produced by FBK and employed for calorimetric applications at moderate neutron fluences were irradiated at LNL up to 10^{11} n/cm^2 (1 MeV eq). The dark current increases by two order of magnitude when the neutron fluence goes from 10^9 to 10^{11} n/cm^2. The single photoelectron sensitivity is lost at a fluence above 3×10^9 n/cm^2. Still, the photosensors can be safely operated in calorimetric mode. An irradiated board of nine 1 mm^2 SiPMs with 15 μm pixel size retains sensitivity to the mip if the number of photoelectrons per mip is $\gtrsim 50$. At the maximum fluence (1.2×10^{11}n/cm^2, 1 MeV eq.), the relative response of the UCM to electrons and mips is compatible with the response before irradiation.

Acknowledgments

This project has received funding from the European Union's Horizon 2020 Research and Innovation programme under Grant Agreement no. 654168 and no. 681647. The authors gratefully acknowledge CERN and the PS staff for successfully operating the East Experimental Area and for continuous supports to the users. We thank L. Gatignon, M. Jeckel and H. Wilkens for help

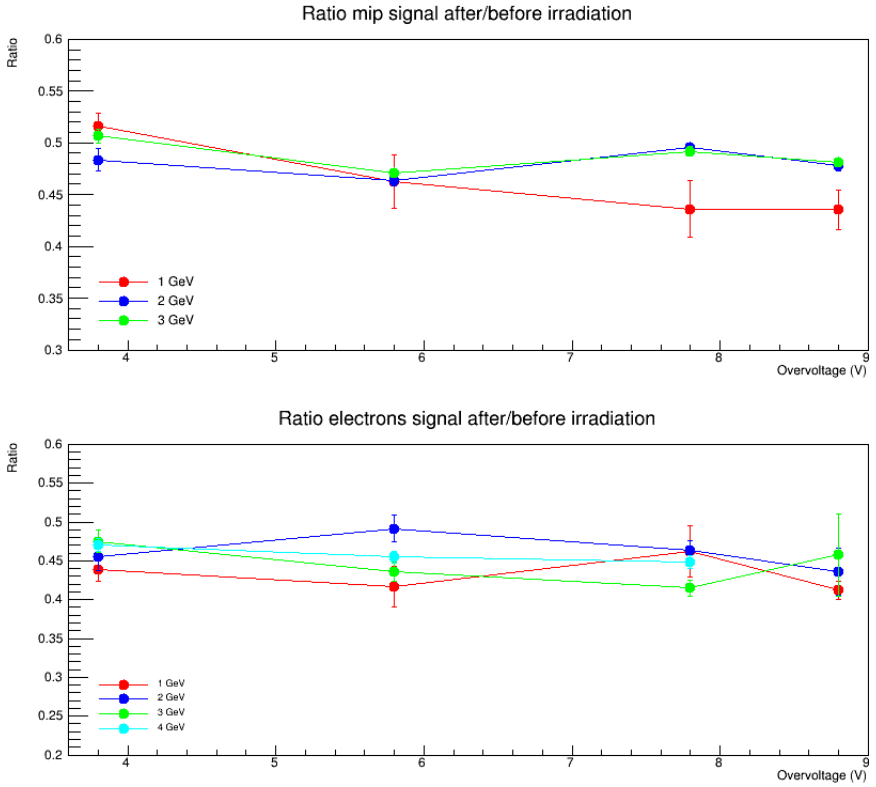

Figure 13: Ratio between the mip (upper plot) and electron (lower plot) peak signal amplitude after and before irradiation at different energies and overvoltage for 17UA.

and suggestions during the data taking on the PS-T9 beamline. We are grateful to the INFN workshops of Bologna, Milano Bicocca and Padova for the construction of detector and to A. Bau and G. Pessina for support during the installation of the SiPM.

References

[1] C. Adloff et al. [CALICE Collaboration], *Construction and Commissioning of the CALICE Analog Hadron Calorimeter Prototype, JINST* **5** (2010) P05004.

[2] A. Berra et al., *A compact light readout system for longitudinally segmented shashlik calorimeters, Nucl. Instrum. Meth. A* **830** (2016) 345.

[3] Y. Musienko, A. Heering, R. Ruchti, M. Wayne, Y. Andreev, A. Karneyeu and V. Postoev, *Radiation damage in silicon photomultipliers exposed to neutron radiation,* JINST **12** (2017) no.07, C07030.

[4] M. Cordelli, E. Diociaiuti, R. Donghia, A. Ferrari, S. Miscetti, S. Müller and I. Sarra, *Neutron irradiation test of Hamamatsu, SensL and AdvanSiD UV-extended SiPMs,* JINST **13** (2018) no.03, T03005

[5] M. Centis Vignali, E. Garutti, R. Klanner, D. Lomidze and J. Schwandt, *Neutron irradiation effect on SiPMs up to* $\Phi_{neq} = 5 \times 10^{14}\ cm^{-2}$, doi:10.1016/j.nima.2017.11.003 arXiv:1709.04648 [physics.ins-det].

[6] C. Xu, R. Klanner, E. Garutti and W. L. Hellweg, *Influence of X-ray Irradiation on the Properties of the Hamamatsu Silicon Photomultiplier S10362-11-050C,* Nucl. Instrum. Meth. A **762** (2014) 149

[7] E. Garutti, R. Klanner, S. Laurien, P. Parygin, E. Popova, M. Ramilli and C. Xu, *Silicon Photomultiplier characterization and radiation damage investigation for high energy particle physics applications,* JINST **9** (2014) C03021.

[8] A. Berra et al. [ENUBET Collaboration], *Enabling precise measurements of flux in accelerator neutrino beams: the ENUBET project,* CERN-SPSC-2016-036; SPSC-EOI-014.

[9] P. W. Cattaneo, T. Cervi, A. Menegolli, M. Oddone, M. Prata, M. C. Prata and M. Rossella, *Radiation Hardness tests with neutron flux on different Silicon photomultiplier devices,* JINST **12** (2017) no.07, C07012

[10] A. Heering, Y. Musienko, R. Ruchti, M. Wayne, A. Karneyeu and V. Postoev, *Effects of very high radiation on SiPMs,* Nucl. Instrum. Meth. A **824** (2016) 111.

[11] A. Longhin, L. Ludovici and F. Terranova, *A novel technique for the measurement of the electron neutrino cross section, Eur. Phys. J. C* **75** (2015) 155.

[12] H. Fessler, P. Freund, J. Gebauer, K. M. Glas, K. Pretzl, P. Seyboth, J. Seyerlein and J. C. Thevenin, *A tower structured scintillator lead photon calorimeter using a novel fiber optics readout system, Nucl. Instrum. Meth. A* **228** (1985) 303.

[13] G. S. Atoyan et al., *Lead-scintillator electromagnetic calorimeter with wavelength shifting fiber readout, Nucl. Instrum. Meth. A* **320** (1992) 144.

[14] A. Berra *et al.*, *Shashlik Calorimeters With Embedded SiPMs for Longitudinal Segmentation,* IEEE Trans. Nucl. Sci. **64** (2017) no.4, 1056.

[15] F. Acerbi, G. Paternoster, A. Gola, V. Regazzoni, N. Zorzi, C. Piemonte, *High-Density Silicon Photomultipliers: Performance and Linearity Evaluation for High Efficiency and Dynamic-Range Applications* IEEE J. Quantum Elect. **54** (2018) 4700107.

[16] G. Ballerini *et al.*, *Testbeam performance of a shashlik calorimeter with fine-grained longitudinal segmentation,* JINST **13** (2018) P01028

[17] D. Bisello *et al.*, *LNL irradiation facilities for radiation damage studies on electronic devices,* Nuovo Cimento **C38** (2015) 189

[18] S. Agosteo *et al.*, *Characterization of the energy distribution of neutrons generated by 5 MeV protons on a thick Beryllium target at different emission angles,* Appl. Rad. Isot. **69** (2011) 1664.

[19] T.T. Böhlen, F. Cerutti, M.P.W. Chin, A. Fassò, A. Ferrari, P.G. Ortega, A. Mairani, P.R. Sala, G. Smirnov and V. Vlachoudis, *The FLUKA Code: Developments and Challenges for High Energy and Medical Applications,* Nuclear Data Sheets **120** (2014) 211

[20] A. Ferrari, P.R. Sala, A. Fassò, and J. Ranft, *FLUKA: a multi-particle transport code,* CERN-2005-10 (2005), INFN/TC_05/11, SLAC-R-773.

[21] Advansid s.r.t., Via Sommarive 18, I-38123, Povo, Trento, Italy

[22] Y. Qiang, C. Zorn, F. Barbosa and E. Smith, *Radiation Hardness Tests of SiPMs for the JLab Hall D Barrel Calorimeter,* Nucl. Instrum. Meth. A **698** (2013) 234

[23] `http://sba.web.cern.ch/sba/BeamsAndAreas/East/East.htm`

[24] ELJEN Technology, 1300 W. Broadway, Sweetwater, TX 79556, USA

[25] KURARAY CO., LTD., Ote Center Building,1-1-3, Otemachi, Chiyoda-ku, Tokyo 100-8115, Japan

[26] Uniplast OOO, Vladimir, st. Bolshaya Nizhegorodskaya, 77, Russia,

[27] S. Agostinelli et al. [GEANT4 Collaboration], *GEANT4: A Simulation toolkit, Nucl. Instrum. Meth. A* **506** (2003) 250.

[28] J. Allison et al. [GEANT4 Collaboration], *Geant4 developments and applications*, *IEEE Trans. Nucl. Sci.* **53** (2006) 270.

[29] J. Allison et al., *Recent developments in Geant4, Nucl. Instrum. Meth. A* **835** (2016) 186.